6 An electrowetting phenomenon: the lensing effect

In the preceding chapters, we explored the static and dynamic wetting of droplets; however, for application purposes, controlling droplets on (super)hydrophobic surfaces is crucial. In this chapter, we choose the electrowetting on dielectric (EWOD) technique to manipulate droplets. Infact, the droplet's spherical curvature at the interface can act as a liquid lens. We investigate the immiscible liquid-liquid interface as an adjustable lensing platform based on EWOD, highlighting on a planar liquid lens experiment and a numerical simulation of an adaptive liquid lens using COMSOL Multiphysics® software.

6.1 Introduction

In this chapter, we explore the control of liquid droplets on solid surfaces using the electrowetting technique. Electrowetting offers a dynamic approach to manipulate liquid behavior through an applied electric field [32]. Many researchers have applied the principles of electrowetting-on-dielectric (EWOD) to manipulate droplets on natural leaves and bioinspired artificial surfaces [95–97]. In addition to these surfaces, electrowetting on (super)hydrophobic dielectric-coated electrode surfaces has been widely studied with growing interest [106, 227, 228]. Various methods exist for controlling droplet dynamics and transitions, including the application of electric fields, magnetic fields, pressure, thermal gradients acoustic, and mechanical stress [30, 229, 230]. Among these, electrowetting has garnered significant attention due to its versatility and wide range of applications, particularly in guided droplet transport, droplet splitting and merging, and digital microfluidic platforms, such as lab-on-a-chip devices and optical liquid lens systems [231–233]. The increasing interest in devices based on EWOD principles is largely driven by their unique advantages, such as low power consumption, fast response time, and broad tunability [32, 234].

In optical lensing, liquid lenses are emerging as a fast-growing technology in

optofluidic devices [99, 234, 235]. Conventional optical lenses, typically made of glass or specialized transparent polymers, face limitations in mechanical focal length adjustments. In contrast, liquid lenses offer rapidly adjustable focal lengths by changing the liquid-liquid interface shape of the lens [236]. Electrowetting liquid lenses are highly valued for a broad spectrum of practical applications, including artificial eyes in robotics, optical switches, and cameras [234, 237–240]. Similar to traditional glass microlenses, electrowetting microlenses, which consist of two immiscible liquids, allow the focal length of the liquid–liquid interface to be adjusted by applying an electric field, thereby altering the interfacial curvature [99]. Earlier, various types of liquid lenses, such as microdroplet planar lenses and adaptive liquid lenses, have been demonstrated with voltage-controlled variable focal lengths [99, 234, 235, 241, 242].

In this study, we explore two aspects of electrowetting: (i) an experiment on planar liquid lenses and (ii) a numerical simulation of adaptive liquid lenses using COMSOL Multiphysics®. In the planar liquid lens experiment, silicone oil and Johnson's® mineral oil served as insulating liquids, with a droplet of KCl saltwater as the conductive liquid. Increasing voltage caused the static contact angle of the droplet to decrease until contact angle saturation (CAS) is reached, altering the liquid-liquid interface curvature and focal length of liquid lens. Additionally, we carried out a simulation study on an adaptive liquid lens utilizing the EWOD principle. The model consisted of three insulating liquids contained within a cylindrical chamber coated with hydrophobic materials with varied thickness, Parylene-C and Teflon-AF. The simulation revealed that applying a voltage above a certain threshold transitioned the lens from a diverging to a converging state, demonstrating the influence of voltage on both focal length and curvature switching.

6.2 Planar lens of two immiscible liquids

6.2.1 Material and methods

The EWOD experiments were carried out with two insulating oil media independently: silicone oil (99.9%, Merck®) and commercially available Johnson's® mineral oil. The density of oil was measured from the mass-volume ratio: the density of silicone oil was $\sim$0.968 g/cm^3 and Johnson's mineral oil $\sim$0.797 g/cm^3. Also, the refractive index (n) of the oil used was measured with the help of a digital refractometer (Holmarc Opto-Mechatronics® Ltd.), with values $n \sim 1.410$ (silicone oil) and $n \sim 1.4589$ (Johnson's® mineral oil). Here, $\sim$0.01 M KCl salt water has been used as a conducting liquid droplet. The volume of the conducting liquid droplet was kept at $\sim 5\ \mu$L.

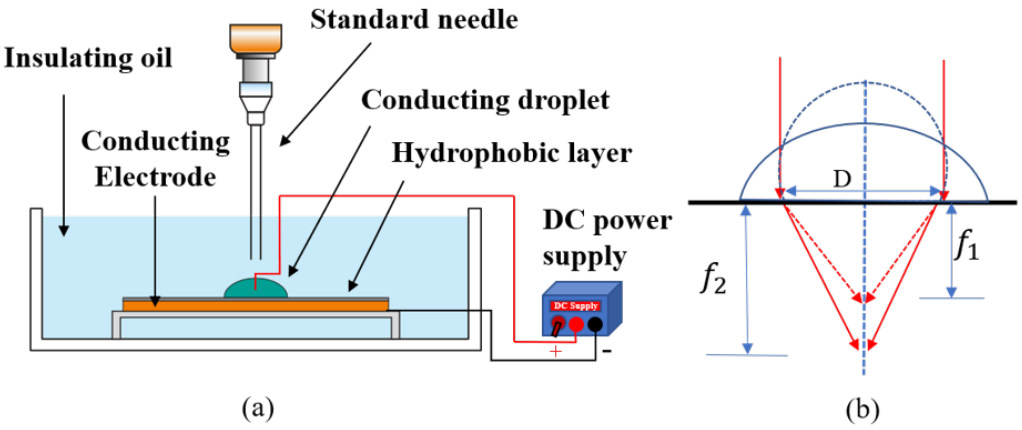

Figure 6.1: (a) Schematic diagram of the EWOD experimental setup. (b) Conducting droplet shape change of the liquid lens. After the application of a dc voltage, the conducting droplet becomes more flattened and the focal length changes from f_1 to f_2.

6.2.1.1 Dielectric film deposition

Poly (vinylidene fluoride-hexafluoropropylene) with a molecular weight of 400,000 (PVDF-HFP, 99.9%, Sigma Aldrich®) was dissolved in acetone (99.9%, Merck®) at room temperature by constant stirring (∼300 rpm). A 10 wt.% PVDF-HFP solution was utilized to prepare a hydrophobic thin film coating on the electrode using the dip-coating technique, with a constant immersion and retraction speed of ∼5 cm/min. The substrates were dried at a fixed temperature of ∼80° C for 12 h.

6.2.1.2 Electrowetting experiment

The static CA measurement was conducted using a contact angle meter (*Kyowa Interface Science Co., Ltd.*). The schematic diagram of the EWOD setup is shown in Fig. 6.1(a). The applied voltage on the saltwater droplet results in a decrease in the contact angle. Consequently, the oil-salt droplet interface becomes flatened compared to the case when no voltage is applied. The schematic in Fig. 6.1(b) illustrates the variation in focal length corresponding to the change in the curvature of the interface. In the EWOD setup, a variable DC power supply offering a stable voltage magnitude from ∼0 to 300 V is required. The DC power supply voltage range depends on the value of the dielectric thickness. Here, the deposited PVDF-HFP ($\varepsilon_r = 10$) thin film thickess of ∼8 μm taken for the entire experiment.

6.2.2 Results and discussion

6.2.2.1 Voltage dependent contact angle measurements

First, we conducted a static contact angle characterization using EWOD. The Fig. 6.2 optical image of the voltage-dependent droplet in an oil medium illustrates how the

CA changes with the applied voltage. The Figs. 6.2(a_1-a_4) and Figs. 6.2(b_1-b_4) show droplets in silicone oil and Johnson's mineral oil media, respectively, corresponding to different applied voltages. The EWOD response, the variation of CA with applied voltage in silicone oil and Johnson's mineral oil is shown in Fig. 6.3(a). A change in the contact angle can be defined in terms of the electrowetting number (η) (see Eq. 2.33), which is given by [32];

$$\eta = \frac{\epsilon_0 \epsilon_r}{2\gamma_{L_1L_2} d} V^2. \tag{6.1}$$

The electrowetting number, η, against the square of the applied DC voltage (V^2) is plotted in the linear region, from $V = 0$ V to $V = 50$ V, as shown in Fig. 6.3(b).

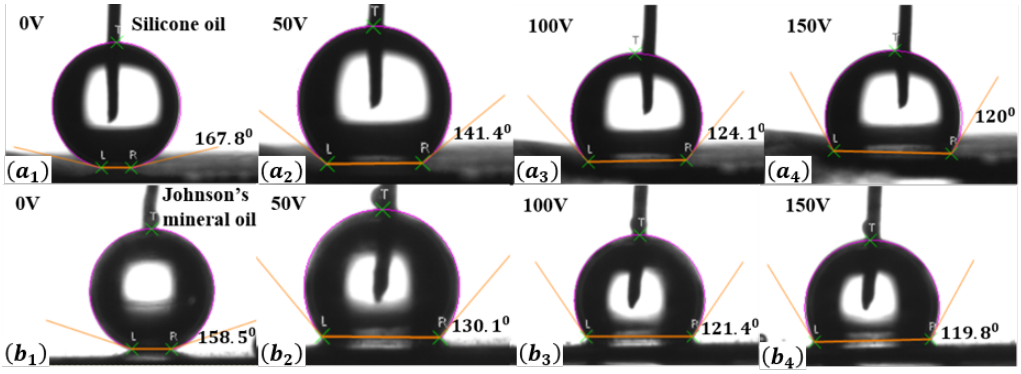

Figure 6.2: Snapshots of EW for two medium silicone oil and Johnson's mineral oil on salt water droplet for increasing voltage magnitude.

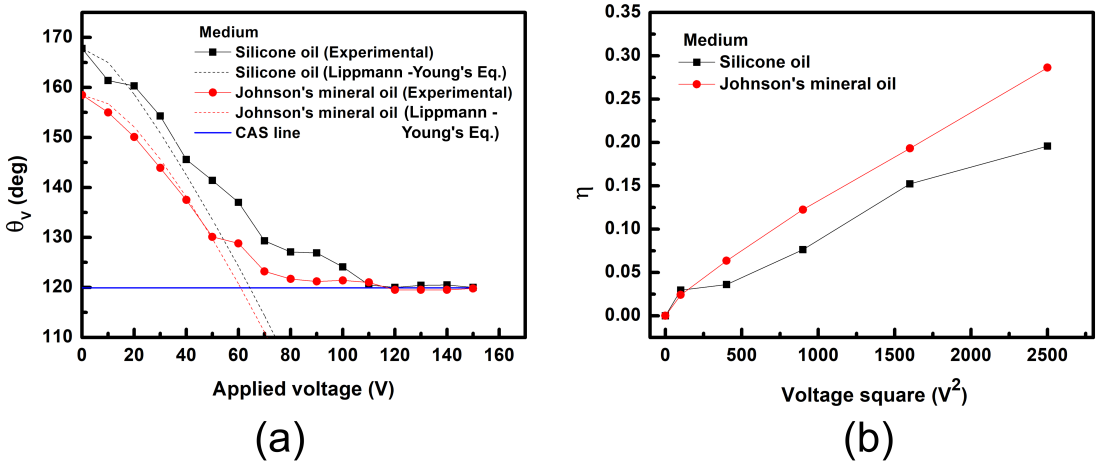

Figure 6.3: (a) EW of two immiscible liquids, the variation of contact angle (θ) as a function of an applied DC voltage for silicone oil and Johnson's mineral oil as a medium. The dashed curves show Lippmann-Young's equation (see Eq. 2.32). At larger voltage, the contact angle becomes saturated (CAS line), $\theta_{\text{Sat}} \approx 120°$. (b) The variation of electrowetting number against applied DC voltage square (V^2) is plotted for $V = 0$ V to $V = 50$ V.

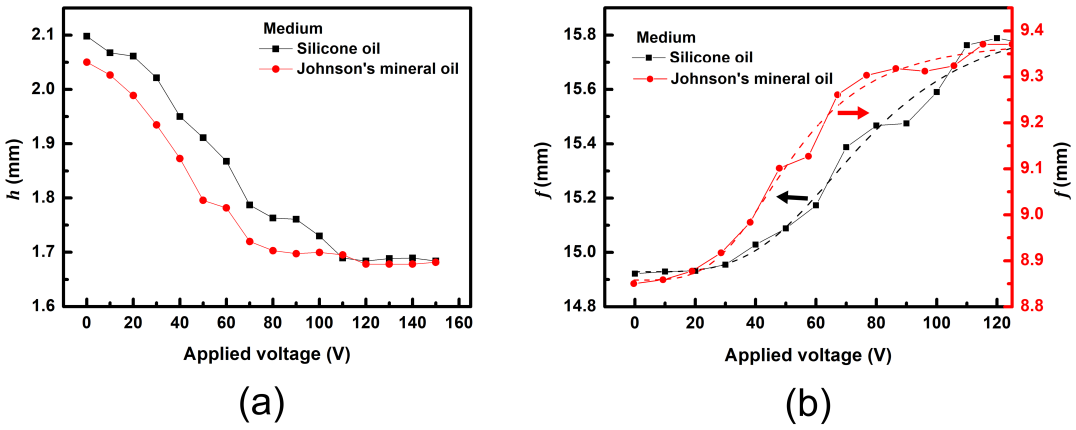

Figure 6.4: (a) Behaviour of droplet height on applied voltage. (b) Plot of focal length versus applied voltage (solid line). The dashed line (non-linear logistic fit) trends of focal length. The arrows direction show axis assigned for curves.

6.2.2.2 Focal length calculation

The variation in focal length with applied voltage is one of the important aspects of this work. Although there are methods to measure the focal lengths of the liquid drop lens, we obtained the focal length by evaluating the radius of curvature of the droplet in response to the applied voltage. A small, spherical liquid droplet forms a spherical cap when it comes into contact with a plane solid surface, for a fixed droplet volume. The liquid droplet may lose or alter its shape due to the effect of gravity. There is a particular length, the capillary length, which estimates the effect of gravity. To eliminate this issue, we used a small droplet volume of 5 μl. Using elementary mathematics, one can derive the relations between the contact angle (CA) and the radius of curvature (R_c) for a fixed droplet volume (V_{drop}) [113].

$$R_c = \left[\frac{3V_{drop}}{\pi(2 - 3\cos\theta_V + \cos^3\theta_V)}\right]^{1/3}, \tag{6.2}$$

where V_{drop} is the droplet volume. Thus, we can calculate the droplet height $h = R(1 - \cos\theta_V)$ and the focal length using the following relationship [243]:

$$f = \frac{D}{2(n_1 - n_2)\sin\theta_V}. \tag{6.3}$$

Here, $D = 2R_c \sin\theta_V$ is the base diameter of a spherical drop cap (Fig. 6.1(b)), n_1 is the refractive index of the oil, and n_2 is the refractive index of the conducting liquid ($n_1 > n_2$).

The variation in droplet height as a function of applied voltage is shown in Fig. 6.4(a). The droplet height decreases rapidly with applied voltage and exhibits a saturation trend in the high-voltage region. The respective droplet height changes

from ∼2.09 mm to ∼1.68 mm and from ∼2.05 mm to ∼1.68 mm for silicone oil and Johnson's mineral oil, respectively, as the voltage is gradually varied from ∼0 V to 150 V. As the contact angle declines with increasing applied voltage, the base diameter of the droplet tends to expand, while the droplet height drops, resulting in an increase in the focal length eventually. The variation in focal length in response to the applied voltage is depicted in Fig. 6.4(b). The focal length changes from ∼14.92 mm to ∼15.78 mm for silicone oil and from ∼8.85 mm to ∼9.37 mm for Johnson's mineral oil. Since the refractive index of silicone oil is slightly lower than that of Johnson's mineral oil, the former case provides a larger focal length under similar conditions. In the high applied voltage range, due to contact angle saturation (CAS), the focal length does not increase with the applied voltage, as the contact angle falls into a saturation region for high voltages (>120V). The plot of focal length is shown (solid line) in Fig. 6.4(b).

6.3 Adaptive liquid lens: A numerical simulation

6.3.1 Model and simulation techniques

In this work, COMSOL Multiphysics® has been employed for the simulation of two immiscible liquids to work as a lens based on EWOD. The lens model is based on two immiscible liquids filled in the lower and upper half parts of a cylindrical chamber, while the inner walls of the chamber are coated with a thin hydrophobic dielectric material as illustrated in Fig. 6.5(a). To avoid the effect of gravity on the shape of the interface, we considered density-matched liquids but of different refractive indices. Moreover, the simulation was performed on three different carefully chosen insulating liquids, namely silicon oil, *n*-hexadecane, and *n*-tetradecane, with two hydrophobic surfaces of Parylene-C and Teflon AF. The simulated results of the EWOD-based adaptive liquid lens with controllable focal lengths are discussed and performance compared for different applied voltage, dielectric types, and layer thickness. Owing to a notable change in any of the parameters, the typical system controls the volume of the two liquid domains proportionately and results in a change in the liquid-liquid interface of the two domains. The change in shape from concave to convex one of liquid-liquid interface results in a profound change in focal length. Furthermore, the effects were analyzed with reference to altered biasing voltages and for different dielectric thicknesses.

6.3.1.1 Geometrical confguration and materials

In the simulation, two-dimensional (2D) axisymmetric geometry has been opted for in place of a 3D model to reduce run time but to acquire analogous results in the

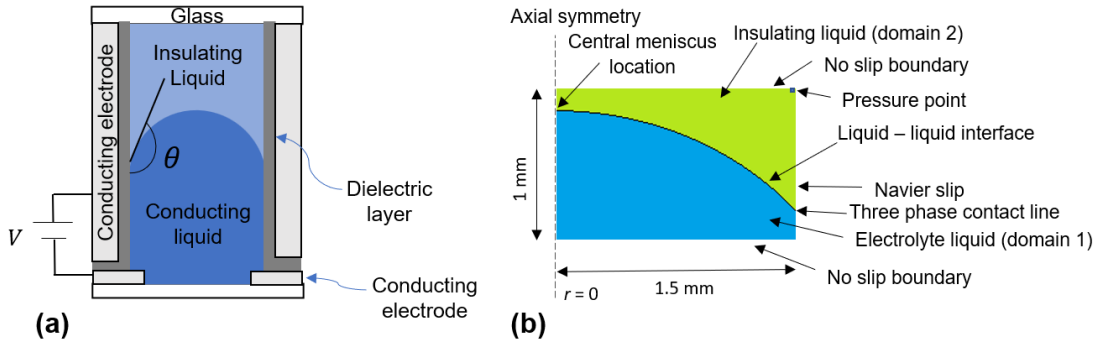

Figure 6.5: (a) A schematic of an EWOD liquid lens system. The liquid-liquid interface showing concave (diverging lens) shape at zero bias voltage. (b) Schematic 2D geometry of the COMSOL modelling. A 2D axisymmetric condition is used and a Navier slip boundary condition is applied to the wall at the contact line with applied voltage. Only the right-half part of the liquid interfacial layer is illustrated.

former case. This also help track the location of the liquid-liquid interface of the two liquids within domains and predict velocity and pressure fields. Typically, two immiscible liquids, namely conducting aqueous potassium chloride (KCl) solution and silicone oil, filled in two domains of diameter 3.0 mm and a height of 1 mm, have been used (Fig. 6.5(b)). The inner wall of the cylindrical chamber was believed to be coated with a hydrophobic material to help the electrolytic liquid reduce its contact area while the insulating liquid oil has an increased surface area. As a result, the conducting liquid makes a convex shape at the liquid-liquid interface and a flexible convex lens with varied focal lengths. To be mentioned, the inputs were chosen from the reported experimental works available in the literatures [244–247]. The two different hydrophobic materials used here are namely, Parylene-C and Teflon AF and that the hydrophobicity of the former can efficiently be controlled by O_2 plasma treatment. Consequently, the water CA of plasma-treated Parylene-C is close to super-hydrophobicity and approximately, 140° [248]. In contrast, the reported CA on Teflon AF is about 120° [249, 250]. Also, a 0.0214 M KCl solution of density 998.1 kg/m^3, and dynamic viscosity 0.8907 mN/m has been employed so that the electrolytic liquid droplet CA is close to the water CA [251]. The interface of electrolytic liquid in conjunction with one of the three insulating liquids (silicone oil, *n*-hexadecane, and *n*-tetradecane) has been examined through simulation (Table 6.1).

Above all, a laminar two-phase flow moving mesh interface model is configured for tracking the location of the interface by a moving mesh, with appropriate boundary conditions imposed by surface tension and wetting [252–254].

Table 6.1: Physical parameters of insulating liquids used in the simulation

Insulating liquid	Density, ρ (kg/m^3)	Dynamic viscosity, η (mPa-s)	Water interfacial tension, γ (mN/m)	Refractive index, n_1	Reference
Silicone Oil	**930.0**	**9.30**	**41.30**	**1.403**	[244]
n-Hexadecane	**772.53**	**3.446**	**54.95**	**1.434**	[245, 246]
n-Tetradecane	**763.09**	**2.3037**	**52.25**	**1.429**	[245, 247]

6.3.1.2 Governing equations: Navier-Stokes (N-S) theorem

The flow of liquids as a relationship between momentum and pressure and within individual domains and phases can be expressed by using the Navier-Stokes (N-S) equation. The general isothermal N-S equations can be stated as [255]:

$$\rho\left(\frac{\partial \mathbf{u}}{\partial t} + (\mathbf{u}\cdot\nabla)\mathbf{u}\right) = \nabla\cdot(-p\mathbf{I}' + \tau) + \mathbf{f}, \tag{6.4}$$

$$\frac{\partial \rho}{\partial t} + \nabla\cdot(\rho\mathbf{u}) = 0, \tag{6.5}$$

where ρ is mass density, $\mathbf{u}$ is vector velocity, p is scalar pressure field, τ is the viscous stress tensor for the Newtonian liquid with dynamic viscosity η [256], $\mathbf{I}'$ is the identity matrix, and $\mathbf{f}$ is the volume force vector. The Eq. 6.4 essentially depicts the rate of change of momentum and characterizes Newton's second law of motion, whereas the continuity equation (Eq. 6.5) describes the conservation of mass. In this simulation, we take the Mach number, $M_c < 0.3$, which implies the incompressible nature of the liquid ($\nabla\cdot\mathbf{u} = 0$). The validity of boundary conditions for the two liquid-liquid interfaces is specified by the "no-slip" criterion between the liquids at the solid boundary wall, and for the liquid-solid wall, the "Navier slip" condition is expected [254, 257, 258].

6.3.2 Results and discussion

6.3.2.1 Effect of applied voltage on lensing

Subject to the adequate electric potential applied across the electrodes, an electric double layer (EDL) develops which could bring a change in the surface tension of the liquids. Consequently, the nature of the dielectric surface may switch from hydrophobic to hydrophilic for the electrolytic liquid, but hydrophilic to hydrophobic for the insulating liquid, giving out an effective concave lens at the liquid-liquid interface. The situation was meant for an insulating liquid of silicon oil, a 4 μm thick layer of hydrophobic Parylene-C, and with the effect of voltage being captured for a time span of $t = 0.05$ s to adjudicate how the liquid-liquid interface changes with the biasing voltage. It may be noted that, the nature of the interface (converging, or diverging) will invariably alter in response to the applied voltage for a given set of im-

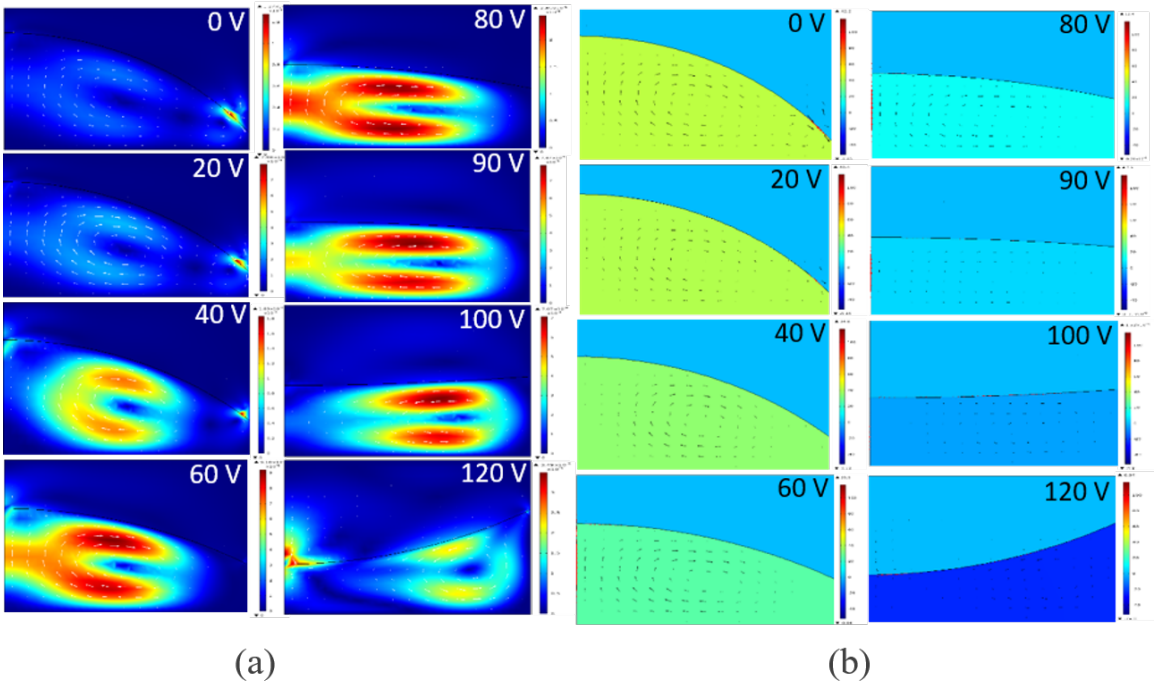

Figure 6.6: The position variation of the liquid–liquid interface with (a) liquids velocity magnitude (m/s) (colour), and (b) pressure magnitude (Pa) (colour) and their direction (arrows) in response to different applied voltages (set time, $t = 0.05$ s) with 4 μm thick Parylene-C hydrophobic surface layer.

miscible liquids and hydrophobic layer. The location of central meniscus height and three-phase contact line corresponded to radii $r = 0$, and $r = 1.5$ mm, respectively. To a great extent, the interfacial shape is now dictated by the applied voltage. The typical voltage-dependent velocity and pressure profiles of the interface leading to the EWOD liquid lens are shown in Figs. 6.6(a) and 6.6(b), respectively. Referring to an immiscible silicone oil-electrolytic interface and with a hydrophobic layer of Parylene-C, Fig. 6.6 clearly show smooth transition of concave to convex shape taken at increasing voltage from 0 V to 120 V. One can notice the shape-changeover from concave to convex lensing effect at critical applied voltage exceeds 95.2 V.

The simulation was performed considering three insulating liquids such as, silicon oil, *n*-hexadecane, and *n*-tetradecane, and with two hydrophobic surface-types, Teflon AF and Parylene-C. As evident from the velocity as well as pressure profiles, the contact angle (CA) and hence the focal length are profoundly dependent on the applied voltage. The declining trends of CA in response to the applied voltage as predicted for different pairs of immiscible liquids and two hydrophobic layer types are depicted in Figs. 6.7(a, c). On a comparative note, silicone oil offers a diverging to converging transition at a relatively lower biasing voltage of 96.5 V and 95.2 V for Teflon AF and Parylene-C hydrophobic layer thickness of 4 μm respectively. Interestingly, the use of *n*-hexadecane and *n*-tetradecane display similar trends for such a switching phenomenon, but at higher critical voltages, i.e., 111.4 V and 108.6

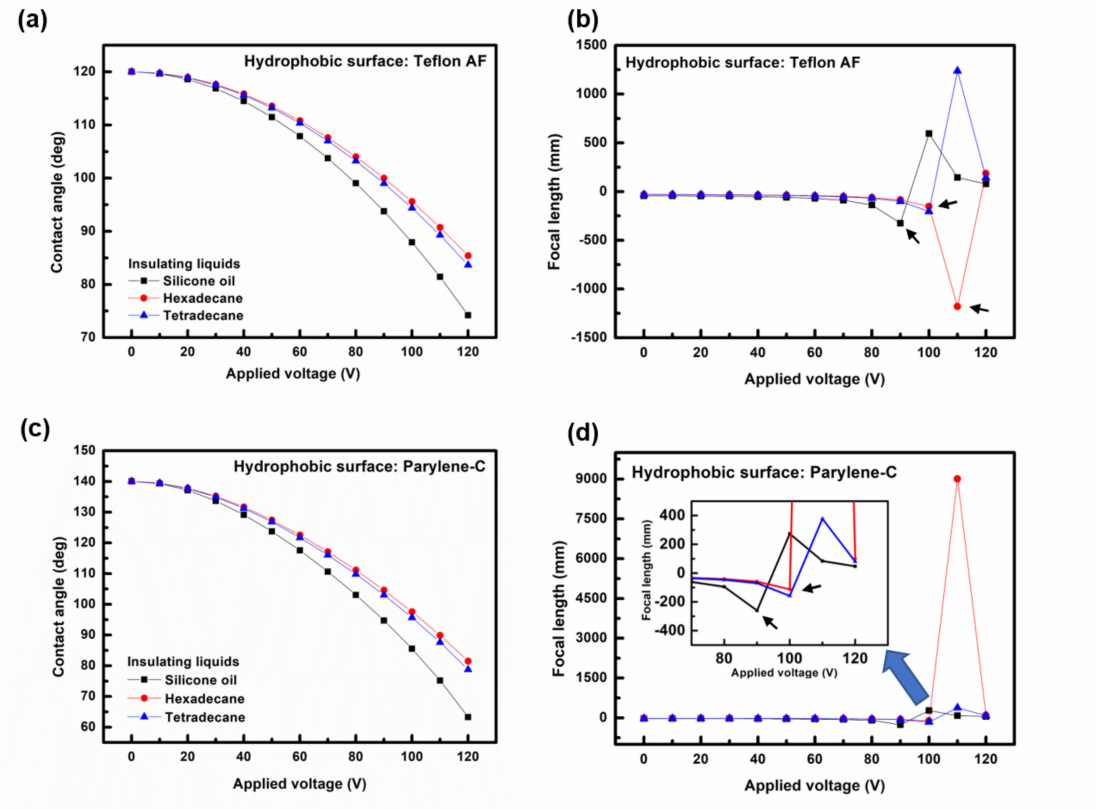

Figure 6.7: The contact angle and focal length plot as a function of applied voltage for two hydrophobic surfaces with the dielectric layer thickness of 4 μm. The sub-figures (a), and (b) are meant for Teflon-AF, while (c), and (d) for Parylene-C (t = 0.05 s). The short arrows in (b, d) essentially represent the flipped state of the liquid interface.

V for Teflon AF, 109.8 V and 107.1 V for Parylene-C respectively, than the case for silicone oil. Accordingly, distinct CA features and altered foci can be ensured. An augmented biasing voltage flips the concave interface into a convex shape, with an observable sign change of focal length, from negative to positive (Figs. 6.7(b, d)). The focal length is determined through the following relationship [259]:

$$f = \frac{r}{(n_1 - n_2)\cos\theta}, \tag{6.6}$$

where r is the radius of the cylindrical lensing system, $n_1 (> n_2)$ is the refractive index of the insulating liquid, and n_2 is the refractive index of the conducting liquid ($n_2 = 1.333$) [259]. Here, $r = \pm R\cos\theta$, with respective signs '+' for obtuse ($\theta > 90°$) and '-' for acute ($\theta < 90°$) angles, R being the radius of curvature. Thus, focal length can be redefined in the following form [243]:

$$f = \frac{R}{(n_1 - n_2)}. \tag{6.7}$$

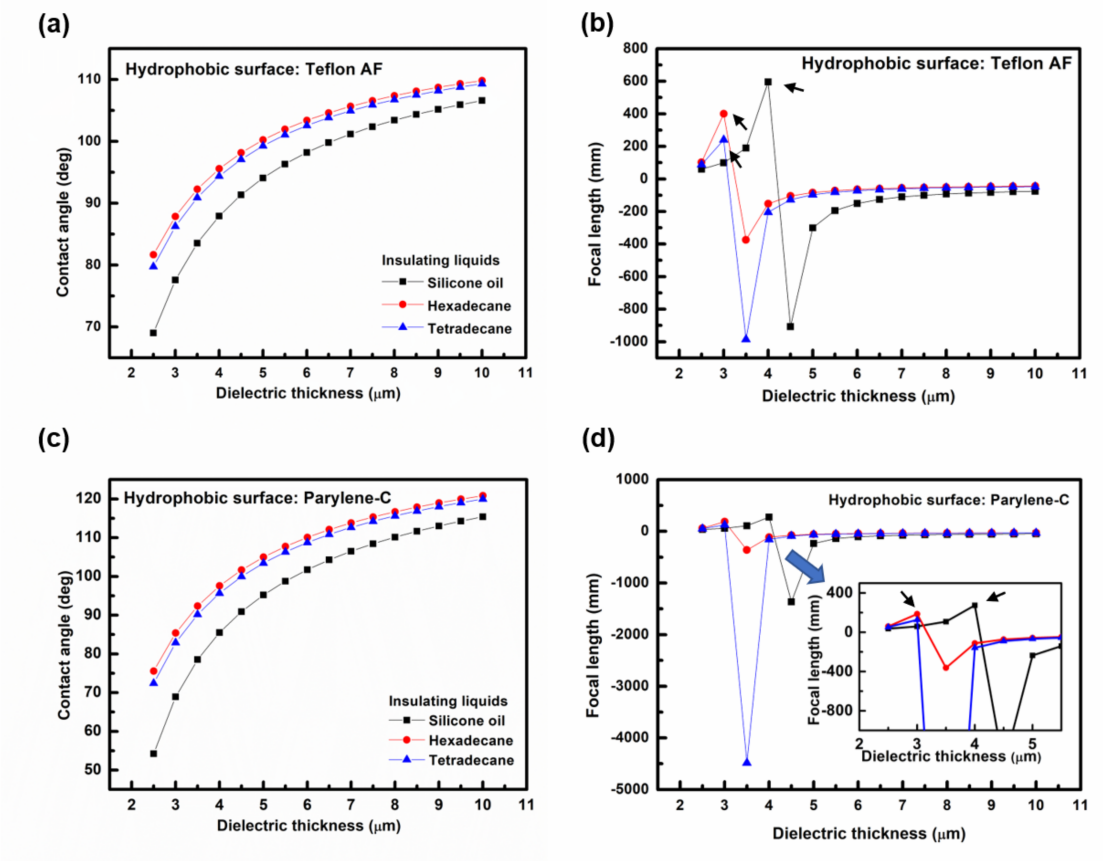

Figure 6.8: The contact angle and focal length as a function of dielectric thickness for two dielectrics Teflon- AF and Parylene-C hydrophobic surfaces shown in figure (a), (b) and (c), (d) respectively. All the trends correspond to a fixed critical voltage of 100 V (t = 0.05 s).

6.3.2.2 Effect of hydrophobic layer thickness on lensing

The aforesaid discussion was based on a hydrophobic layer of fixed thickness of 4 μm. The effect of layer thickness on the CA of a given pair of immiscible liquids, as well as the predicted focal distance around the critical voltage (in this case, 100 V), are shown in Fig. 6.8. In this regard, the hydrophobic layers of Teflon AF ($\epsilon = 2.0$) and Parylene-C ($\epsilon = 3.15$) with thicknesses of 3 μm to 4 μm were seen to favor the lensing effect, i.e., converging to diverging nature (Fig. 6.8). The abrupt change in EWOD-based liquid lens focal lengths as a consequence of the difference in the refractive indices of the two liquids is more prominent for silicone oil and n-tetradecane cases (Figs. 6.8(b, d)). By changing the hydrophobic thickness slightly from 2.5 μm to 4.5 μm, the focal length becomes more positive, and further increasing it turns the lens more negative (as indicated by short arrows in Figs. 6.8(b, d)), with the meniscus shape switching over from a converging to a diverging lens. Subjected to a non-zero biasing voltage above the critical value, one can easily tune the liquid lens of the desired type by changing the dielectric layer thickness.

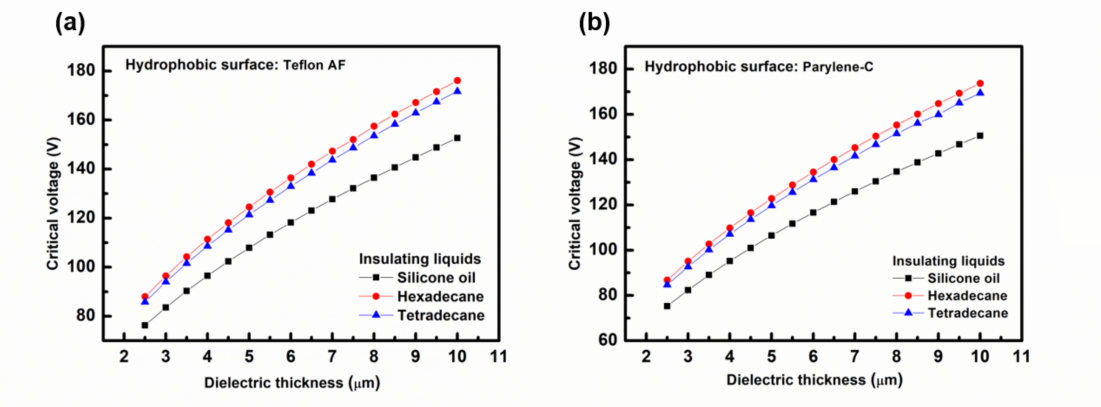

Figure 6.9: Plots for critical voltage as a function of coated dielectric layer thickness for different insulating liquid-KCl pairs: (a) Teflon AF, and (b) Parylene-C hydrophobic dielectric surfaces.

6.3.2.3 Effect of critical voltage and dielectric thickness

One of the most important parameters in the EWOD system is the critical voltage as it dictates the switching of the liquid lens from the convex to concave shape on a hydrophobic surface of finite thickness. As can be noticed from Fig. 6.8, a step of 0.1 V above the critical voltage is likely to flip the nature of focal length, converting diverging to converging lens-type. The critical voltage vs. dielectric thickness of Teflon-AF and Parylene-C hydrophobic surfaces can be found in Fig. 6.9. Generally, a lower critical voltage is anticipated to make the setup more versatile and technically reliable. However, it is limited by the hydrophobic layer thickness and a given set of immiscible insulating-electrolytic liquid pairs. For a given dielectric layer thickness, the critical voltage remains low for the silicone oil-KCl pair as compared with other liquid pairs (Fig. 6.9). To be mentioned, an extremely thin dielectric layer does not warrant true hydrophobic feature while a very large thickness may attract a penalty of working at a higher critical voltage therefore, a carefully chosen dielectric thickness is desired for the proper functioning of the device.

The prime challenge is to keep the critical voltage as low as possible so that the liquid lens experiences a swift transition from concave to convex one. On the other hand, a thin dielectric layer may not necessarily be a hydrophobic to help sustain the interfacial layer created by two immiscible liquids. From the analysis of Figs. 6.7, 6.8, and 6.9, it is quite apparent that the silicone oil-KCl interface is a better candidate over others as there is a possibility of a smooth transition in this case at a relatively lower voltage. Conversely, *n*-hexadecane and *n*-tetradecane insulating liquids demand a higher voltage to establish the lensing feature. Nevertheless, they provide higher focal lengths as compared with silicone oil-KCl-based immiscible liquids.

6.4 Conclusion

To conclude, the experimental conditions and important findings are as follows.

1. Planar liquid lens: experimental study

- Insulating media: Johnson's mineral oil and silicone oil.
- Conducting liquid: KCl salt water.
- Focal length range:
  (i) Silicone oil: ∼14.92 mm to ∼15.78 mm.
  (ii) Johnson's mineral oil: ∼8.85 mm to ∼9.37 mm.
- Voltage range: ∼0-120 V.

2. EWOD-based adaptive liquid lens simulation

- Chamber: Cylindrical, 3.0 mm diameter, 1.0 mm height.
- Hydrophobic surfaces: Parylene-C and Teflon-AF.
- Insulating liquids: Silicone oil, *n*-hexadecane, and *n*-tetradecane.
- Conducting liquid: KCl salt water.
- Voltage effect:
  (i) Liquid curvature switches from diverging to converging one for voltages greater than ∼90 V.
  (ii) The focal length varies approximately within the range of ±400 mm, with a discontinuity occurring near the voltage at which the curvature flips from concave to convex type as the applied voltage increases from 0 to 120 V.